



Operational performance and grid-support assessment of distributed flexibility practices among residential prosumers under high PV penetration



Yanxue Li ^{a,*}, Xiaoyi Zhang ^b, Weijun Gao ^{a,b}, Wenya Xu ^a, Zixuan Wang ^a

^a Innovation Institute for Sustainable Maritime Architecture Research and Technology, Qingdao University of Technology, Qingdao, 266033, China

^b Faculty of Environmental Engineering, The University of Kitakyushu, Kitakyushu, 808-0135, Japan

ARTICLE INFO

Article history:

Received 27 April 2021

Received in revised form

5 July 2021

Accepted 10 August 2021

Available online 19 August 2021

Keywords:

PV integration

Energy flexibility

Smart meter data

Distributed energy technologies

Grid-support performance

ABSTRACT

This study explores the impacts of increased photovoltaic (PV) penetration on a real-world power grid. Detailed operational scenarios of existing distributed energy technologies, including grid-tied PV, heat pump, micro-cogeneration, and battery systems among smart residential prosumers are examined using smart meter data. Then, to quantify the grid-support interactions of the decentralized electricity generation and consumption under high grid PV penetration, we introduce grid-support indicators to recognize their induced month-to-month variations based on the dynamic grid spot trading price and carbon emission density profiles. The results show that increased electricity consumption is attractive when the flexible consumption is shifted to a low grid spot trading price and carbon emission intensity period. The grid-support benefits of distributed generators are improved when their output enables a reduction in imported electricity during the grid residual load peak period. The direct simple integration of distributed PV generation makes it difficult to achieve grid-support operation at high solar penetration levels. The analysis results provide insight into the favorable scheduling of the heat pump consumption for time periods corresponding to a large quantity of available on-site PV generation to improve the grid-support performance. The results would help policymakers govern grid-support assets more equitably from a system-level perspective.

© 2021 Elsevier Ltd. All rights reserved.

1. Introduction

1.1. Motivation

Renewable energy and energy efficiency improvements are considered key resources for decarbonizing social energy systems [1]. The levelized cost of renewable energy technologies has fallen dramatically, even below the cost for some conventional fossil fuel-based plant generation. The cumulative capacity of installed photovoltaic (PV) and wind generation has rapidly increased globally, and exhibits a continuously rising trend [2,3]. However, the levelized electricity costs may fail to capture the variability or time-varying values regarding the timing match between power generation and end-user load profiles [4,5]. The increased

integration of fluctuating renewable energy supply has led to challenges in the reliability and cost-efficient operation of public grids. For example, the increasing contribution of PVs has caused associated duck curve challenges [6,7], and some PV generation had to be curtailed owing to insufficient grid flexibility at certain times [8]. The large share of intermittent renewable generation has led to the need for electric flexibility to mitigate the variability and uncertainty in demand and generation. Therefore, the transition to carbon neutral energy systems will require more flexible energy use. The ongoing transition of flexible energy systems varied across different regions, and a number of studies have indicated the need for an inclusive approach to ensure that none of the flexible measures is left behind [9–11]. Researchers are focusing more on improving energy flexibility from different perspectives [12,13], and power planning models have demonstrated continuous interest in investing in various flexible technologies [14]. The building sector is a major energy consumer, accounting for approximately 40% of global energy consumption. Energy sector coupling technologies such as decentralized heat pumps and micro cogeneration

* Corresponding author.

E-mail addresses: 15315005563@163.com, liyanxue@qut.edu.cn (Y. Li), yi.619@163.com (X. Zhang), gaoweijun@me.com (W. Gao).

systems are gaining popularity, and result in the opportunity to harness more flexibility in aggregated form [15,16]. The exploration of the cost competitiveness alternatives of energy flexibility from demand-side efforts is attracting increasing attention in facilitating the rising variable of renewable integration [17].

Considering the increasing integrated distributed energy resources [18], the coordination between generation and consumption is considered to have a significant impact on the grid available flexibility, and electrical utilities are increasingly considering the integration of demand response measures or technologies as potential flexibility providers, improving their aggregated cost-effectiveness and carbon reduction performances in the operational stages. The increasing market penetration of distributed building energy systems, such as rooftop PV, micro combined heating and power (CHP), and heat pumps, has contributed to the short-term or seasonal variability in both individual household and centralized energy consumption profiles [19]. With the rapid development of advanced metering infrastructure and Internet of Things (IoT) control, it has become possible to distribute prosumers that are compatible with the public grid [20]. The coordinated management and role assessment of real-world distributed flexible practices is becoming important in terms of their flexible operational performance.

1.2. Literature review

The capital cost of distributed PV and battery technologies has experienced a rapid decline over the last decades, and this has led to an increased cumulative installed capacity [21,22]. There is already empirical evidence that the initial integration of variable renewable generation has been favorable in lowering the grid marginal electricity generation cost, which is commonly known as the merit order effect [8,23]. However, the market value of variable renewable energy tends to decline as its proportion rises further [24,25], and previous works have verified that high penetration levels of PV integration have led to PV curtailment in an effort to stabilize the public grid operation, thus influencing the cost-effectiveness of variable renewable integration [8]. Research has already indicated that the aggregated incentive demand response could modify the pattern of the power load profile [26], and the associated impacts of optimally distributed flexible practices cannot be neglected [27].

The current building sector is experiencing increasing electrification; in turn, aggregated flexibility from demand-side energy management is expected to benefit from the increasing integration of available renewable energy [28]. To capture the variable cost and to stabilize grid operation, different electricity tariff schemes in the residential sector were introduced by electricity companies to foster active demand-side energy conversion and load shift willingness activities, inducing the reshaping of the aggregated electricity consumption profile together with the grid flexibility requirement [29,30]. These energy prosumers may be encouraged to delay or force the operation of the energy device in response to different external electricity price signals, such as time of use, real-time pricing, and upstream charge tariffs [17,18,31], voluntarily modifying their short-term energy usage patterns. Meanwhile, price-responsive load scheduling is expected to be a cost-efficient approach to providing deliverable energy flexibility and offering potential energy cost savings from the coordinated management of distributed energy systems [32,33].

For the end-user side, given the intensive growth of smart home appliances, distributed PV, battery storage, heat pumps, and micro CHP systems, it attracted increased attention in activating demand-side flexibility to accommodate increasing shares of the variable renewable energy generation as well as providing energy cost

savings [34]. The rapid development of advanced information and communication technologies (ICTs), which accelerates grid-supportive demand response issues, presents an opportunity to manage and optimize decentralized energy devices [15,35]. Demand-side management has attracted much attention in dealing with real-time energy imbalances as well as grid ramp variability [35]. For example, grid interactive efficient and energy-flexible building concepts were discussed, aimed at providing price-responsive flexibility for grid service, while co-optimizing energy cost for flexible energy consumers [36,37]. Meanwhile, rising energy sector coupling adds more complexity to district energy systems; grid-support buildings that consider managing the fluctuations in load and available generation are becoming an alternative to grid-flexible investment. If distributed generators are not properly organized, it may further increase the supply-demand imbalance. Therefore, there is a need to acquire a better understanding of the operation of existing flexible technologies and to quantify the potential grid-support benefits that could be harnessed from the demand side.

In accordance with the importance of demand-side management, many governments have encouraged the development of smart low-carbon or nearly zero-energy buildings to achieve a high self-consumption ratio of on-site renewable generation and to enable grid-support participation in the aggregated form [33,38]. Currently, the grid-service role from the active management of building energy stores and releases has also been highlighted to accelerate the transition to a low-carbon grid [39–41]. The coordinated integration and control of distributed heat pumps, thermal storage, and micro CHP systems have attracted increasing attention as system-friendly resources to deal with the real-time mismatch between energy production and consumption profiles [42,43]. A number of studies have verified the role of optimized grid-connected batteries with bidirectional power flows in increasing local PV self-consumption [27]. Previous work has also introduced the potential for the bottom-up modeling of distributed hybrid PV-battery systems in flattening the public grid load [44], enabling the participation of grid-supportive battery dispatch as peaking load resources [45], and reducing system generation cost [46]. Thermal energy storage coupled with heat pumps or micro CHP systems is becoming a popular alternative to distributed flexibility. The effectiveness of optimal control on the flexible thermal load was confirmed by maximizing the integration of renewable energy generation [47]. In combination with thermal storage units the use of heat pumps has increased the feasibility of demand response insight into energy conversion and load shifting [48]. The power to heat (P2H) approach with proper management is highlighted as a cost-attractive solution to absorb excess renewable generation or to fill valley load by optimizing the daily flexible operation of heat pumps, while improving the local PV self-consumption ratio [49,50]. Vijay, Avinash, and Adam Hawkes [51] evaluated the performance when using decentralized residential heating systems as a low-cost and flexible alternative to absorb surplus renewable generation, and the results indicated that the heat pump can effectively shift electricity consumption into an off-peak period. The CHP system features a more controllable power output compared with variable renewable generation, especially when coupled with a thermal storage unit. Nuytten et al. [52] assessed the available flexibility of CHP coupled with thermal storage based on the extent to which energy use can be delayed or forced compared with the initial load profile. Demand-response programs such as real-time price enabled building CHP systems to adjust their operational conditions regarding supply-demand balance, providing energy flexibility and cost-saving benefits [53]. With respect to the duck curve challenge, Takeshita, Takuma, et al. [54] reported the effectiveness of aggregated distributed micro-CHP in

offering flexible support for the public grid. A summary of common flexible options is illustrated in Table 1.

To date, it has been simple to define the energy flexibility of large-scale energy systems [34,59], and different performance indicators have been introduced, such as storage capacity, dispatch efficiency [34], local self-consumption ratio [60], duration capacity [61] and carbon emission reduction [62]. Energy efficiency is not a simple integration of on-site renewable or efficient generators because their flexible dispatch may be influenced by many variables, such as weather conditions [48] and occupancy characteristics [63]. Previous assessments focused more on evaluating the contributions of different measures when minimizing system costs and carbon emissions. Dynamic flexibility assessments of existing distributed flexible options in the building sector are generally limited by the absence of historical operational data. It should be noted that diverse energy storage or load shifting technologies feature different configurations and technological parameters, enabling them to have different load shifting abilities that vary from several minutes to days [64]. The differences in the contribution of decentralized flexibility options to public grid operations are generally not well understood. Furthermore, flexibility features an inherent time-coupling characteristic; the continuously increasing integration of variable renewable generation would significantly reshape the pattern of residual grid load, thus influencing marginal power supply cost, and the associated grid flexibility requirement is also evolving. There is a need to assess the extent to which grid-supporting flexibility is available from coordinated distributed technologies management, such as real-time energy load shifting, energy conversion, and co-production by on-site generators. Most studies have failed to capture the evolution of the grid flexibility, leading to an unfair role comparison of diverse distributed technologies under high renewable penetration from a system level. It appears feasible to fill the gap based on the existing smart meter and high-quality open data of the electrical market.

In particular, this study investigated real-world operational scenarios of existing smart residential hybrid energy supply systems in terms of load scheduling, energy efficiency, and delivered grid-support flexibility. Case studies that involve the use of different flexible technologies have been employed to characterize the energy flexibility. Detailed grid-supporting flexibility properties of existing distributed generators, including grid-tied PV, heat pump, and CHP systems with demand response requests were illustrated and compared, and the potential improvements to grid support operation are proposed. The results would help utilities or policymakers to quantify the value of coordinated distributed flexibility, and the systemic analysis of distributed energy efficient technologies or demand-side management strategies would help policymakers to oversee low-carbon grid transitions more equitably and responsibly. During the transition to low-carbon power systems.

The remainder of the paper is structured as follows: Section 1 introduces the recent research review related to energy flexibility and demand-side management. The data resources and methodology are provided in Section 2. Detailed operational scenarios of the power supply and demand sides, analysis results, and potential

Table 1
Summary of the common flexible options related to grid-support integration.

Main focus	Objective	Authors
Storage dispatch, increasing local PV self-consumption, building to grid	PV and battery storage	Li et al. [44]; A.W. Frazier [45]; Jaglal Dillon et al. [46]
Power to heat, absorb surplus renewable energy, dynamic electricity price	Heat pump and thermal storage	Sandberg Eli et al. [55]; Huang et al. [49]; Vijay A et al. [51]
Demand-side management, building thermal load shifting	Building HVAC system	Tang et al. [56]; Li et al. [57]; Huang et al. [58]
Grid ramp rate, combined heating and power	CHP	Nuytten et al. [52]; Takuma et al. [54]

Table 2
Characteristics of thermal power resources.

Variables	Coal based	LNG based	Oil
CO ₂ emission factor, kg/kWh	0.864	0.430	0.695
Contribution ratio, %	70.7	26.8	2.4

improvements are presented in Section 3. Finally, we conclude the paper.

2. Data and methodology

2.1. Renewable integration

Since 2012, the renewable feed-in tariff scheme accelerated the development of distributed renewable generation in Japan in an effort to replace the contribution from closed nuclear plants. With a firm goal to decarbonize grid electricity, the increasing penetration of integrated variable renewable energy has gradually phased out the contribution from thermal power plants in the public grid. For example, the cumulative integrated PV capacity reached 10,000 MW by the end of 2020 in the Kyushu region, annual average carbon emission factor per electricity unit was decreased to 0.370 kg CO₂/kWh. As the capacity of PV plants increase, the grid duck curve increases the need for flexible power resources to resolve the timing imbalance between electricity demand and integrated PV generation. We observed that the adjustment of the flexible thermal power plant had to be accelerated to tackle the variability in PV generation during sunrise and sunset periods. Current information pertaining to thermal power plants in the Kyushu region is shown in Table 2. A grid-scale pump hydro storage system was explored fully to mitigate the grid congestion during the mid-season, and PV curtailment even occurred to stabilize the operation of the grid. Real-time electricity supply demand data of the public grid were obtained from the Japan Renewable Energy Institute, while the power exchanging price was as low as 0.01 Yen/kWh during the daytime overproduction period [65].

The carbon emission intensity of the grid electricity is a function of the generation source set; detailed carbon emission factors and contributions of different thermal power plants are shown in Table 2. Here, we calculate the time-dependent carbon emission factor of grid electricity generation by summing the multiplied measured proportion of power resources and their individual emission factors; details of carbon emission intensity are shown in Appendix D. The direct carbon emission factor of grid electricity is calculated as follows:

$$C_{el}^i = (C_{el}^{coal} \cdot f_{coal} + C_{el}^{LNG} \cdot f_{LNG} + C_{el}^{oil} \cdot f_{oil}) \cdot P_{thermal}^i / P_{el}^i \quad (1)$$

where C_{el}^i is the carbon emission factor of regional grid electricity at time step i , C_{el}^{coal} is the carbon emission factor of a coal-based plant, C_{el}^{LNG} is the carbon emission factor of an LNG-based plant, C_{el}^{oil} is the carbon emission factor of an oil-based plant, f has a unit of %, and represents the output ratio of each plant. Thus,

$C_{el}^{coal} \cdot f_{coal} + C_{el}^{LNG} \cdot f_{LNG} + C_{el}^{oil} \cdot f_{oil}$ represents the overall direct carbon emission intensity of the thermal power plant, $P_{thermal}^i$ is the output of the thermal plant at time step i , and P_{el}^i is the public grid load at time step i .

2.2. Local grid market data

Nine major regional electric power companies are responsible for supplying electricity to each respective service area in the Japanese power grid. Driven by the feed-in tariff support, cumulative capacity of renewable energy plants experienced a rapid expansion, and power companies cooperate with each other to secure a stable power supply, using approaches such as power exchange among electricity companies [65]. The Japan Electric Power Exchange (JEPX) day-ahead market is a wholesale electricity market whereby power generation companies and retail companies exchange electricity at 30 min intervals for the next day. A bid is made using a price auction system that is based on buying and selling conditions. As illustrated in Fig. 1, the value of real-time electricity generation and flexibility requirements are also reflected by the intraday spot electricity price profile in Kyushu public grid [66]. Details of the daily average market spot prices are presented in Appendix A. The seasonality of power demand as well as the increasing PV generation increased the variations in the power exchange price during the summer period, and the compensation on spot power prices has increased significantly. As shown in Fig. 2, it should be noted that the feed-in tariff for distributed PV systems also presents a decreasing trend. Overall, the integration of the variable PV generation increased the pressure to absorb the variations in the net grid load. The supply and demand sides must work together to explore both long-term and short-term grid flexibility assets to deal with the renewable overproduction problem.

With the widespread application of smart meters among buildings, energy policymakers have been paying increasing attention to encouraging the trade-off of energy efficiency between the public grid and distributed flexible energy prosumers. Meanwhile, in order to accommodate the introduction of increasingly variable renewables and stabilize the grid operation, diverse residential electricity rates, including dynamic price-based and volume-based schemes, were launched for end-users to choose, with the aim of encouraging demand-side investments in distributed flexible options and the coordination of demand-side energy

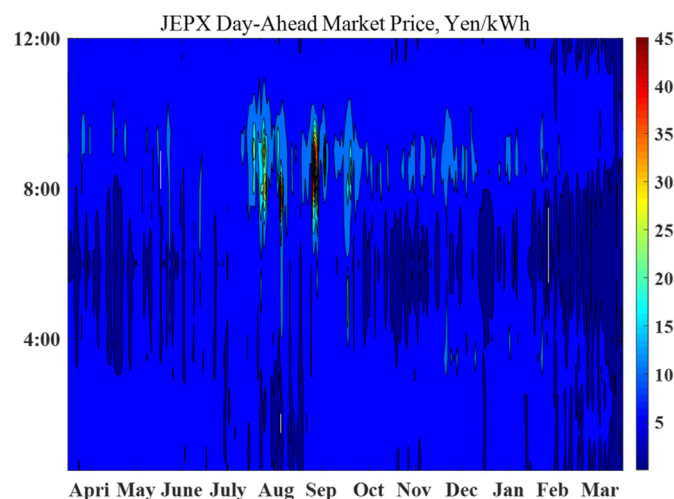


Fig. 1. Annual public electricity intra-day spot pricing profile in Kyushu grid from April 2019 to March 2020 (x-axis: day of the year, y-axis: hour of the day).

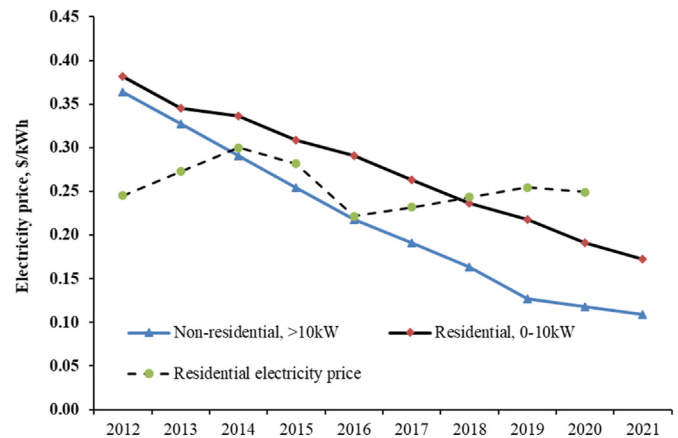


Fig. 2. Historical PV feed-in tariff and average residential electricity price in Japan, resource: Agency for Natural Resources and Energy [65,66].

management.

The energy systems of low-carbon residential houses consist of different distributed energy technologies, and the rooftop solar PV system plays a significant role in increasing local electricity self-sufficiency, while playing a role in cost saving electricity dispatch in terms of the dynamic electricity price. Fuel cell cogeneration systems supply heat and power energy, the heat pump serves as a hot water supplier, and the customer chooses one of them as the home heat resource. We obtained the smart meter data of existing smart Zero-Energy Houses (ZEHs) with representative hybrid energy supply systems located in the Kitakyushu Zero Carbon Demonstration Project, Japan. The selected residential houses, which are equipped with advanced distributed energy technologies, including PV, battery, thermal storage and fuel cell cogeneration systems, and home energy management system (HEMS) as an IoT controller play a key role in optimizing the energy bill of house owners through learning historical operation; meanwhile, it can measure and control in real-time on-site electricity generation and consumption. Table 3 lists the parameters of the selected representative residential energy systems.

2.3. Grid-support coefficients

The optimal scheduling of flexible distributed energy systems, such as rooftop PV, heat pump, micro cogeneration, and battery storage systems can modify the pattern of the residual electricity load. Based on the grid-support coefficient introduced in Ref. [67], we extended the grid-support coefficient indicators to determine the energy cost and carbon emission reduction issues considering the entire energy system. GSC_{cos} represents the relative grid marginal cost support. GSC_{emi} refers to the relative grid carbon emission reduction ability. A large value for distributed generators is favorable as it indicates a relatively lower electricity consumption and high-intensity carbon emissions during the period. In contrast,

Table 3
Information about examined low-carbon residential houses.

Household	Description	Parameters
H1	Heat pump + PV	PV, 6.2 kWp
H2	Heat pump + PV	PV, 6.0 kWp
H3	Fuel cell + PV	PV, 5.3 kWp; Fuel cell, 700 W
H4	Fuel cell + PV	PV, 7.0 kWp; Fuel cell, 700 W
H5	Battery + heat pump + PV	PV, 6.2 kWp; Battery, 6.3 kWh
H6	Battery + heat pump + PV	PV, 6.1 kWp; Battery, 6.3 kWh

for consumers with equipment such as heat pumps, a small value is favorable as it enables them to realize cost-saving and environmental benefits. Details of the local public grid load and PV integration are presented in [Appendix B and C](#). The calculation of the above indicators is based on time-resolved electricity consumption, spot price, and carbon emission profiles.

$$GSC_{cos} = \frac{\sum_{i=1}^n P_{el}^i \cdot C_{el}^i}{P_{el} \cdot \bar{C}_{el}} \quad (2)$$

$$\bar{C}_{el} = \frac{1}{n} \sum_{i=1}^n C_{el}^i \quad (3)$$

$$GSC_{emi} = \frac{\sum_{i=1}^n P_{el}^i \cdot E_{el}^i}{P_{el} \cdot \bar{E}_{el}} \quad (4)$$

$$\bar{E}_{el} = \frac{1}{n} \sum_{i=1}^n E_{el}^i \quad (5)$$

where P_{el}^i in kWh is the generated or consumed electricity in time step i , P_{el} is the cumulative electricity in kWh, E_{el}^i in kg/kWh refers to the value of grid carbon emission in time step i , C_{el}^i in Yen/kWh is the spot price signal in time step i , and n is the total number of time steps.

3. Results and discussion

3.1. Grid operational scenarios

For each month, the scenarios of the daily average grid load and residual electricity demand that minuses the PV integration are shown in [Fig. 3](#). The maximum grid load occurred in August, driven by rising air conditioning consumption. PV generation shares a significant proportion of electricity demand during the daytime. PV integration significantly reshaped the 24-h net grid load curve for each month, and the duck curve was most significant in the mid-season, where the amount of reshaped peak load can increase by as much as three times the minimum residual load that occurs at noon. Therefore, flexible power plants must adjust their output to variations in the feed-in solar production. It is observed that PV production shaves the daytime load in July and August, and the absence of PV production and high grid demand reshaped the peak grid load during the night period, which indicates increasing ramp requirements. The grid valley load decreased further after the integration of PV generation during the daytime in December, January, and February, when there were days with relatively low temperature and increasing heat energy demand in the morning and night periods. At the system level, as a result of a large amount of PV integration, the intraday fluctuations of the residual grid load increased.

[Fig. 4](#) shows the month-specific distributions for the grid spot trading price as well as the carbon emission intensity per electricity unit. The hourly carbon emission profile shows a similar pattern with the residual grid load curve depicted in [Fig. 3](#), the large-scale integration of daytime PV generation has yielded obviously reduced associated CO₂ emission factor per electricity unit. The carbon emission density is relatively high in the winter months owing to the decreased PV production. The minimum carbon emission intensity happens at daytime in mid-season when the PV production shares the largest proportion of the grid demand. The observed spot trading price exhibited a similar trend with net grid demand depicted in [Fig. 3](#). The reduction in the spot trading price

induced by PV integration is large at periods with maximum PV generation in mid-season months, and the minimum value is observed at the noon time in November.

As shown in [Fig. 5](#), in response to the increasing ratio of the daily PV production to grid flexible generation (grid load minus inflexible nuclear power production), the value of the average spot trading price shows an obvious decreasing trend with an increasing PV penetration. Efforts have been made to minimize this effect, and it provides insight into the exploration of demand-side flexibility. The grid-support operation of demand-side participation is related to the electricity used or generated at the right time, which would better reshape the grid on the generation and consumption profile. Therefore, the integration of distributed electricity generation is valuable during periods with high power exchange prices and carbon emission levels, and a shift of the consumer electricity consumption into the off-peak price period is preferred. In the following section, we will examine the detailed operational performance of existing distributed energy technologies based on smart meter data.

3.2. Operational scenarios of demand-side flexible technologies

3.2.1. PV generation and consumption

Generally, a PV system is connected to the public electricity grid via an inverter. Real seasonal and hourly variations of PV integration are shown in [Fig. 6](#), where direct local PV consumption is strongly linked to the temporal coincidence between on-site generation and residential load profiles. We observe that the grid feed-in amount is larger in mid-seasonal months, and the direct self-consumption of PV is high owing to the increased air conditioning and heating demand.

3.2.2. Heat pump utilization profiles

Heat pump water heaters are responsible for the electrification of the residential heat energy consumption. To achieve an adequate exploitation of the dynamic pricing structure (time of use) and meet daily hot water usage, a thermal storage system is equipped to change the method employed in the use of heat energy. The installation of a hot water tank (approximately 400 L) ensures a real-time load shift between hot water pre-generation and heat delivery based on the available electricity tariff. As illustrated in [Fig. 7](#), the implemented rule-based scheduling effectively shifts the operation of the heat pump into fixed hours and avoids the daily peak period of the public grid. Meanwhile, daily hot water generation was determined in the HEMS configuration by setting the starting and finishing times with a maximum amount of price-responsive load shifting. The observed storage duration changed significantly on an intraday and seasonal basis. The full load hours of heat pump pre-generation concentrate in the off-peak price period during the day, and it can also be observed that the power usage varies with the ambient temperature, and cold days drive rising electricity consumption. Their observed ratios of maximum hourly electricity consumption to average electricity consumption are 1.4 (H1) and 1.5 (H2), respectively.

3.2.3. Fuel cell operational profiles

The fuel cell ENE-FARM is the most commonly used micro cogeneration technology in Japanese residential buildings, and enables the simultaneous generation for the residential heat and electricity demand. The nominal power output capacity of ENE-FARM is 700 W, its electricity efficiency is up to 40%, the thermal output is 998 W, the volume of the combined water tank is 130 L, and the temperature of the stored hot water is approximately 60 °C [68]. The operation of the cogeneration system is generally based on the thermal energy following strategy. As shown in [Fig. 8](#), the

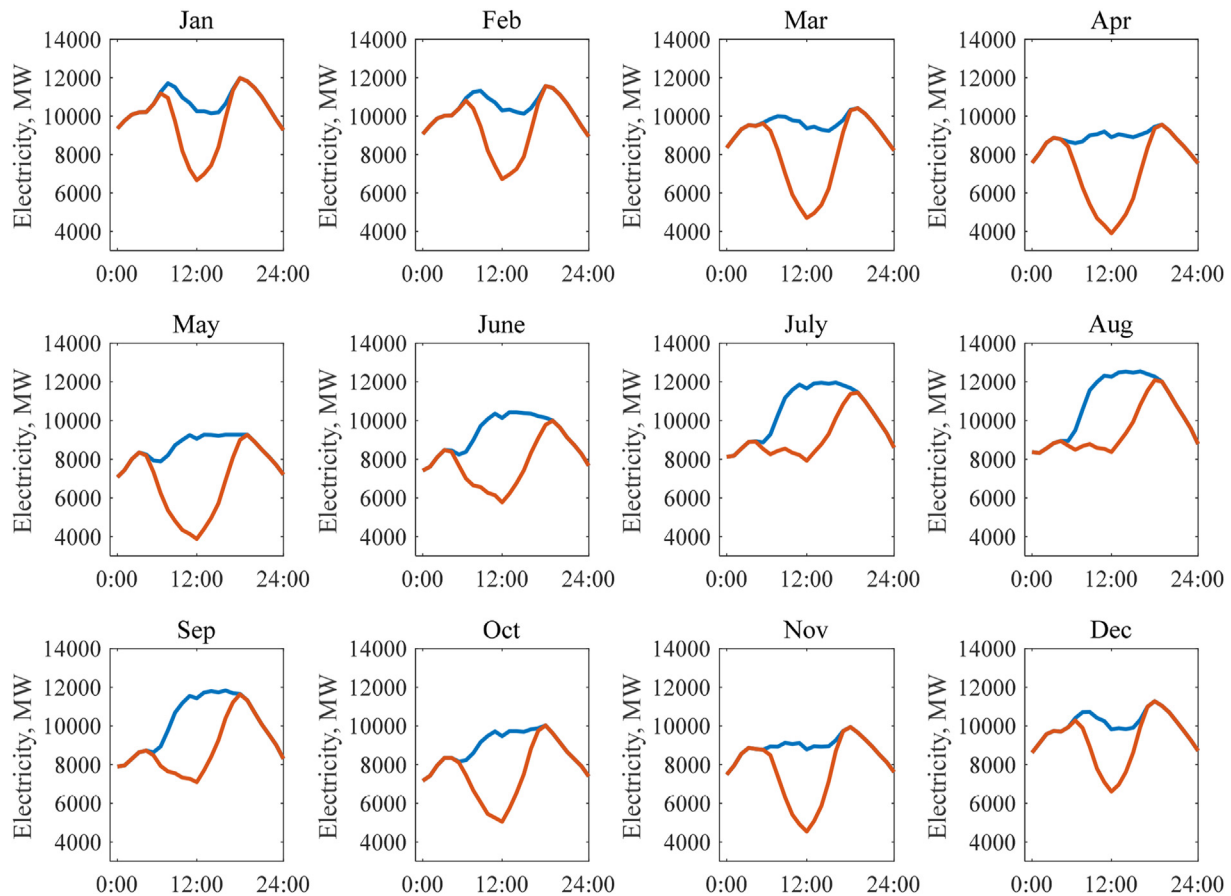


Fig. 3. Average daily grid load profiles and residual grid load profiles minus integrated PV generation for each month. The blue line represents the grid load, and the red line represents the net grid load. (For interpretation of the references to colour in this figure legend, the reader is referred to the Web version of this article.)

measured daily maximum output of the fuel cell is observed primarily when there is no PV output, and its output is limited to the simultaneous heat energy demand, which enables a prolonged working period and increases power generation in winter days. We can also observe that the working period of the fuel cell in H3 has a better correlation with the grid night and morning peak hours.

3.2.4. Battery storage dispatch profiles

The capacity of common home storage battery is about 6.0 kWh, it generally installed to store energy in off-peak price or high PV generation periods. And its charging period generally features short duration and high-power rating. The dynamic battery dispatch scenarios are shown in Fig. 9, where the rule-based control forced the charging process of the battery into the off-peak price period, and it shifted the load upward during this period; then, its discharge process started during night-time peak price hours. The scheduling leads to the peak power load being provided over a shorter period of approximately 3 h, and the discharging flow with a negative value corresponds to the residential peak price period, and the cycling is expected to reduce the power purchased from the utility with a high price under the ToU tariff scheme. The annual cycling efficiencies of the H5 and H6 battery charging-discharging processes were 77.3% and 73.1%, respectively. Overall, battery storage dispatch increased the electricity consumption of households.

3.3. Grid-support performance analysis

Month-specific grid-support coefficients of residential grid-tied

PV systems are shown in Fig. 10, as an electricity producer, high values indicate grid-support integration. It is obvious that their values are high in summer and low in mid-season because the cooling load increased significantly during the daytime in summer, which benefits from a better correlation with the grid load. According to the above analysis, a relatively low residual grid load and decreased value of intraday spot trading price during the PV generation period led to a low value of the grid-support coefficient in the mid-season.

Fig. 11 presents the calculated profiles of the residential heat pump grid-support coefficients. For the consumer, the heat pump load is shifted to the hours with low electricity price time, which generally has the lowest grid load of a given day. The rule-based scheduling of the heat pump has positive effects on cost reduction in winter and summer months in that the value of grid support coefficient is less than 1.0. As a result of the high penetration of the grid PV generation during the daytime, their operational period during night hours is generally associated with a relatively high carbon emission intensity level compared with other periods within a day, and the heat pump thus shown a negative effect on reductions in the operational carbon emission, especially in the mid-seasonal months.

The grid-support coefficients for residential fuel cell systems are shown in Fig. 12. As a producer, the large coefficient values indicate the potential benefits of replacing grid import power. The output profile of the fuel cell in H3 has a similar pattern as that of the spot price and carbon emission intensity curves, yielding a more favorable role in realizing cost and carbon emission reductions compared with H4. The results highlight the impact of the optimal

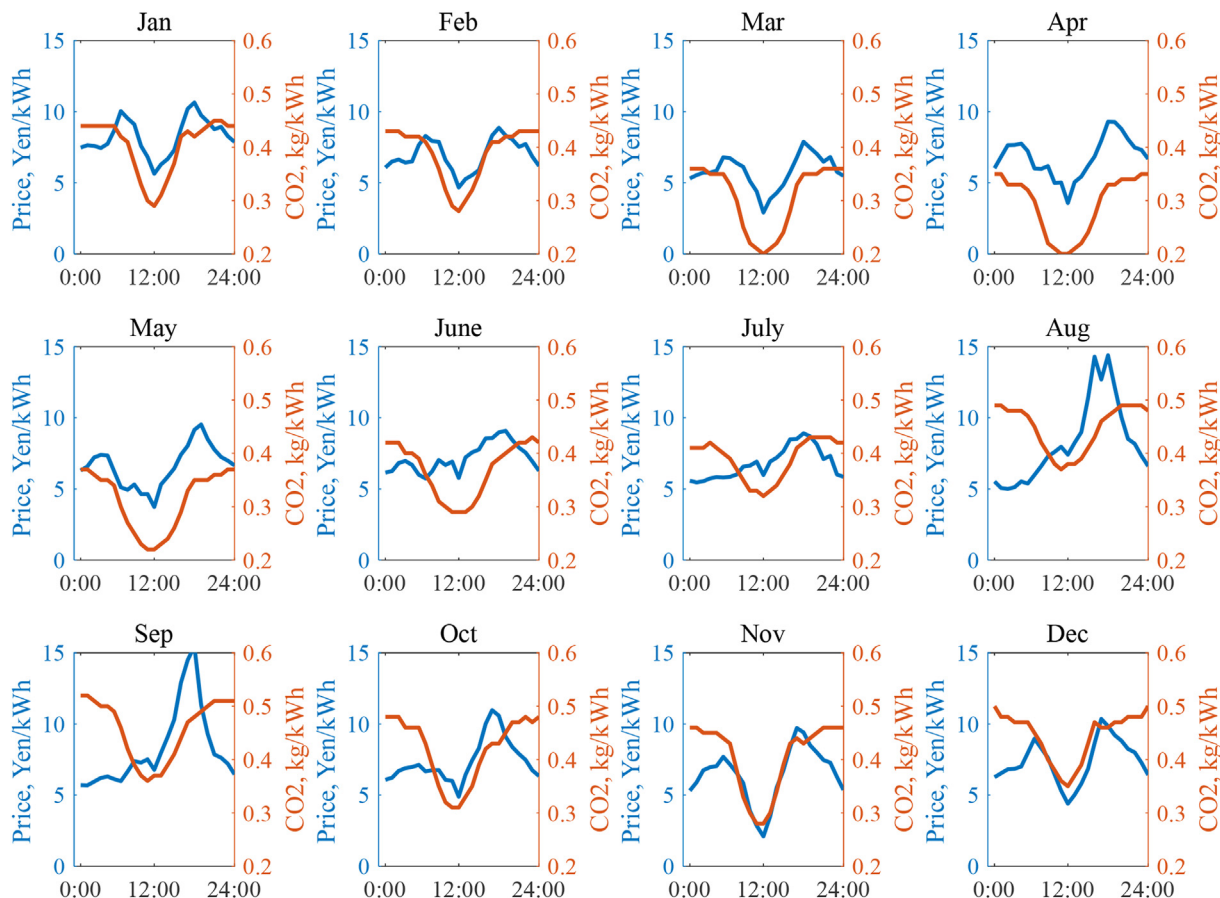


Fig. 4. Average daily grid spot trading price and carbon emission intensity for each month. The blue line represents the spot price and the red line is the carbon emission profile. (For interpretation of the references to colour in this figure legend, the reader is referred to the Web version of this article.)

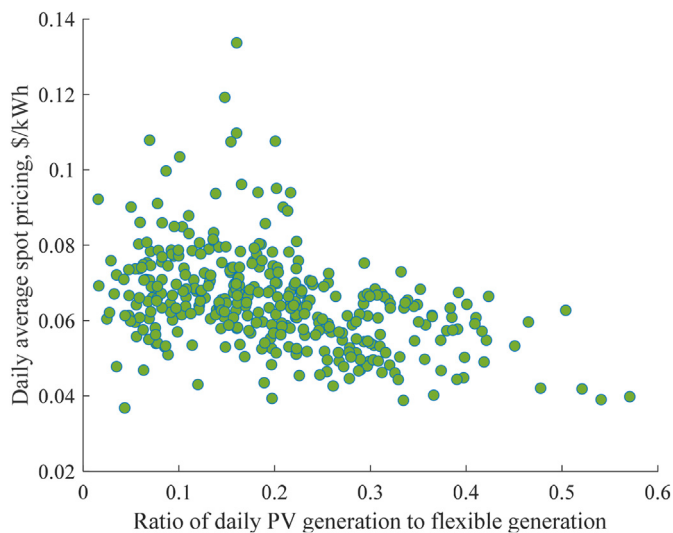


Fig. 5. Scatter distribution of daily average spot price value with ratio of PV generation to grid flexible generation.

scheduling of the cogeneration system on the grid-support performance.

Home battery systems could be considered as an electricity prosumer from a charging-discharging cycle perspective. To calculate the grid-support coefficients, charging consumption and

discharging generation flows are distinguished in negative and positive values, respectively. As shown in Fig. 13 (for H6, the battery is not involved in the load dispatch during October, as shown in Fig. 9), the favorable cost grid-support coefficient is observed from the shifts in the battery load, and a negative value indicates the cost reduction from the cycling dispatch with a high spot price difference between charging and discharging periods. Owing to the cycling energy loss, it failed to yield carbon emission reduction support in all months.

3.4. Demand-side scheduling for improved grid support performance

The direct local PV self-consumption ratio depends largely on the correlation between the PV generation and domestic load profiles. As observed in Fig. 6, a large proportion of daytime PV generation was fed into the grid. Considering the continuously decreasing value of the PV feed-in tariff and grid daytime over-production challenge, it enables an opportunity to increase in the daily PV self-consumption ratio through the optimal scheduling of the heat pump's starting time. As illustrated in Fig. 14, orange dash curve presents PV generation, the grey box depicts the heat pump power consumption, local PV self-consumption marked by grey area can possibly be increased by shifting heat pump's operation into maximum PV generation period. Taking H1 as a study case, the operation period of the heat pump was concentrated in the early morning, and hot water was generated and stored in the tank. According to the daily average PV generation and heat pump

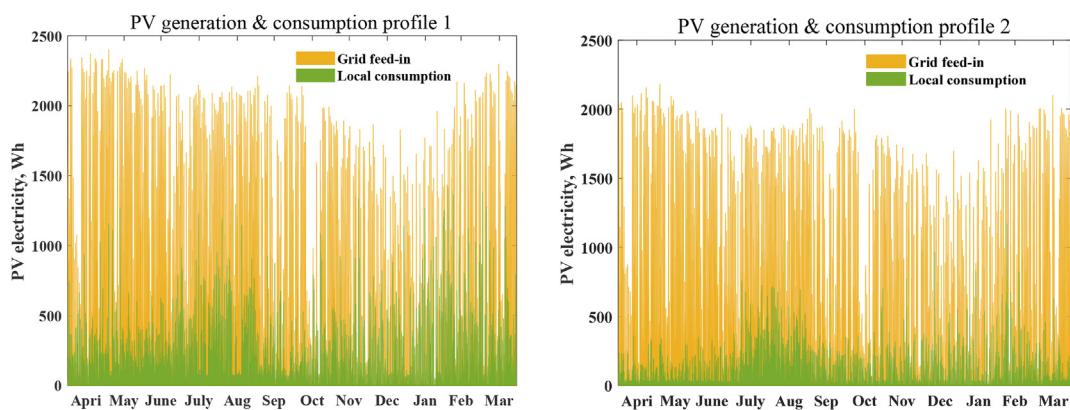


Fig. 6. PV generation and local direct consumption profiles of H1 and H2.

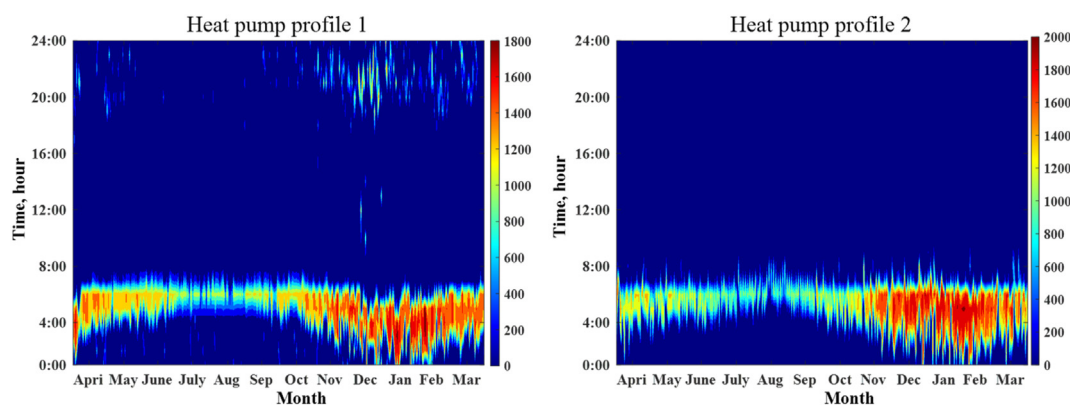


Fig. 7. Heat pump electricity consumption profiles of H1 and H2.

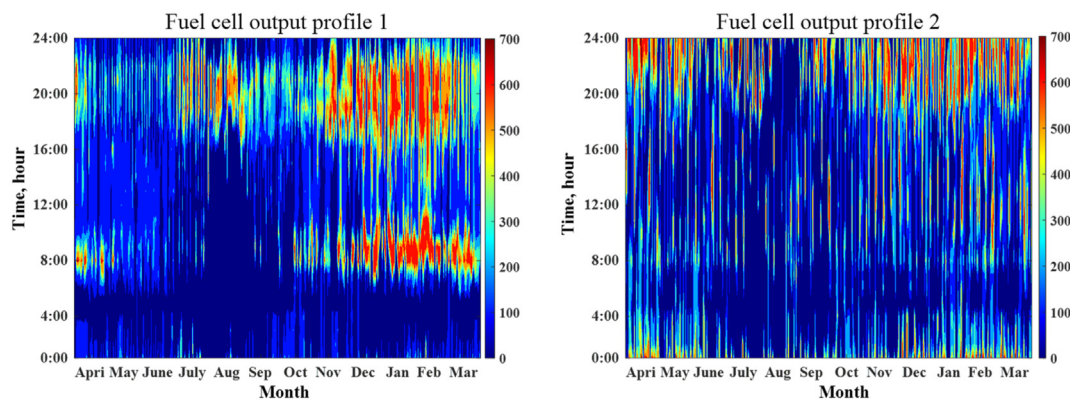


Fig. 8. Fuel cell power output profiles of H3 and H4.

consumption profiles for each month, we determined the heat pump's delayed time in n hours by maximizing the PV self-consumption ratio. The calculation result found that the operational period of the heat pump was delayed by approximately 10 h and shifted to the daytime. Numerical changes in PV self-consumption ratio for each month are illustrated in Fig. 15, and because of the lower generation ability in winter months, most PV generation could be consumed directly and achieved high self-consumption ratios. The heat energy demand is lowest in summer, and scheduling the heat pump system has a limited impact on increasing the PV self-consumption ratio. The load shift of the heat pump system plays a positive role in increasing the PV self-

consumption degree during the mid-season periods.

The above load shifting adds the heat pump load to times of high on-site PV electricity generation, and less electricity will be sold to the grid. As a result, the residential electricity load would be significantly reshaped. To assess the effects of the scheduling of the heat pump system on the grid-support performance, we calculated the grid-support coefficients of the residential consumption profiles before and after power-to-heat load shifting. Detailed month-to-month changes are reflected in their ratio (grid support coefficient value of load shifting divided by the original value), as shown in Fig. 16. This indicates favorable load-shifting effects when the value of the ratio is less than 1.0. Because the daytime spot price is

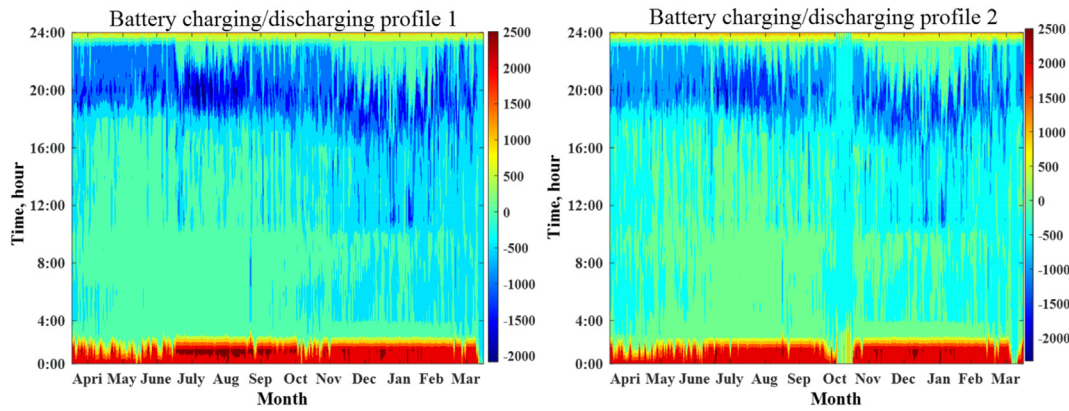


Fig. 9. Battery storage charging-discharging dispatch power flow profiles of H5 and H6.

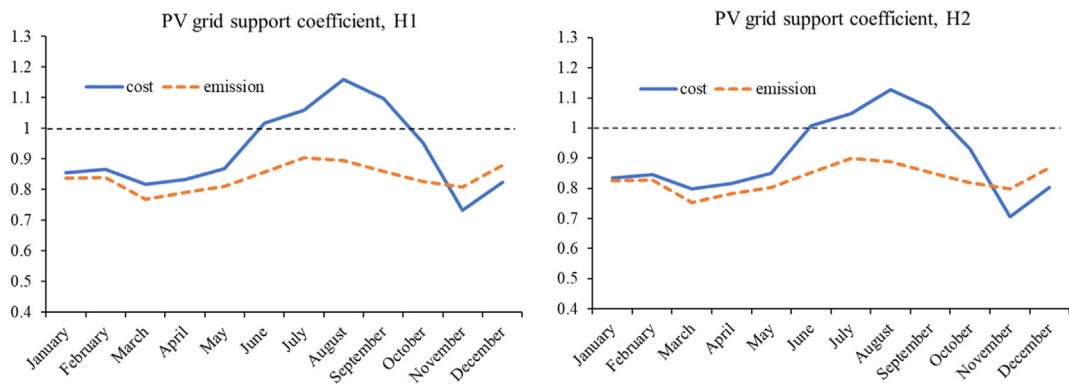


Fig. 10. Month-to-month grid-support coefficients of residential rooftop PV systems.

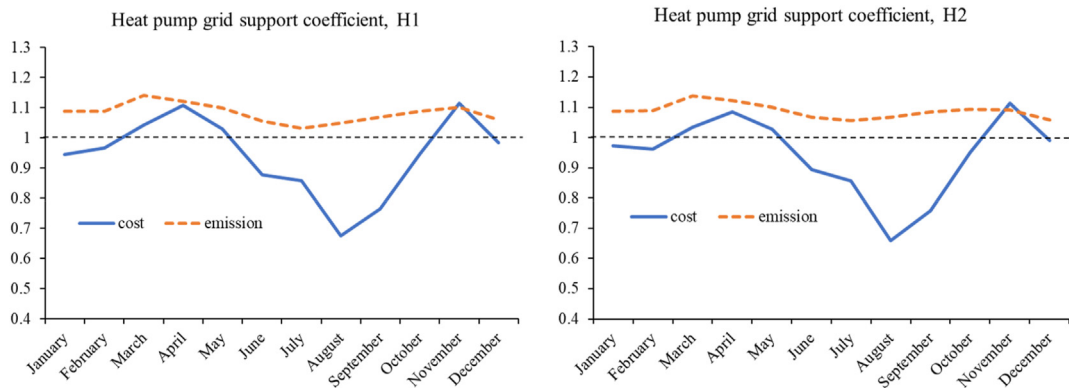


Fig. 11. Month-to-month grid-support coefficients of residential heat pump systems.

higher than in the early morning in summer, the scheduling of the heat pump is unfavorable for improving the cost grid-support coefficient. The scheduling reduces the grid feed-in PV flow in mid-season times, and improved grid-support effects are clearly observed. The combination also reduces the carbon emission production in each month at the system level, indicating the need to

manage heat pump scheduling in mid-season times.

3.5. Discussion and limitation

The deep decarbonization and efficient management of low-carbon social energy systems require the harnessing of energy

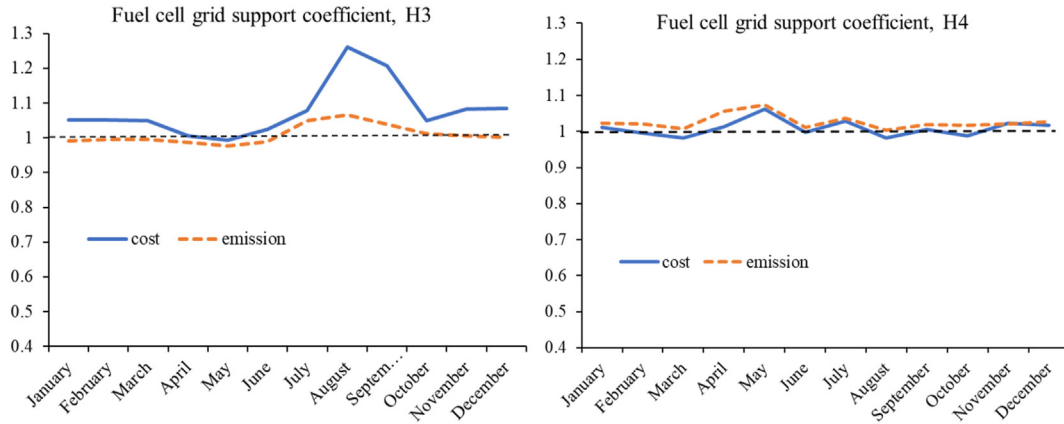


Fig. 12. Month-to-month grid-support coefficients of residential fuel cell systems.

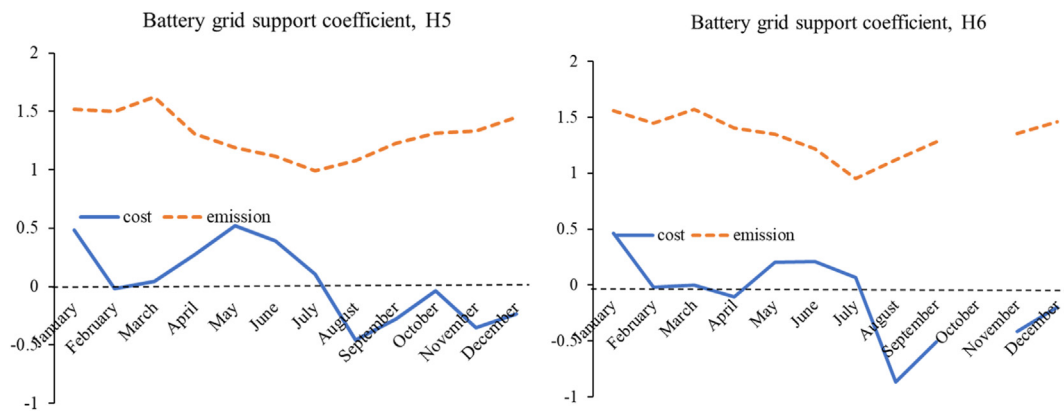


Fig. 13. Month-to-month grid-support coefficients of residential battery storage dispatch systems.

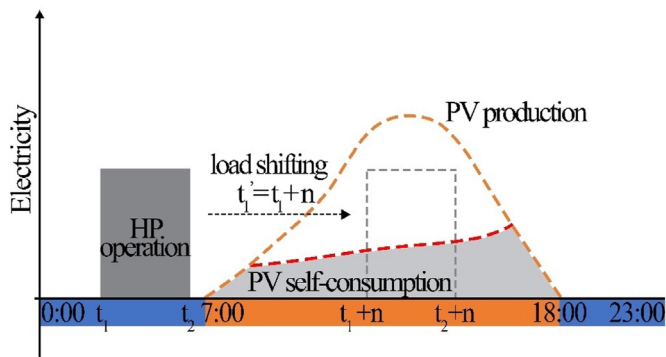


Fig. 14. Load shift of heat pump to increase local PV self-consumption.

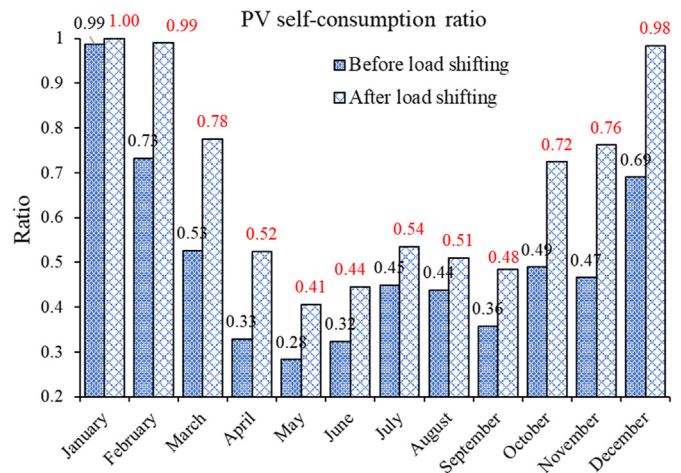


Fig. 15. Changes of PV self-consumption ratio in each month after scheduling heat pump systems.

flexibility from the end-user side. Currently, grid-tied distributed PV technology is a mature application, and the installed capacity has an increasing trend. According to the above analysis results, there is also the potential room for improvement of decentralized

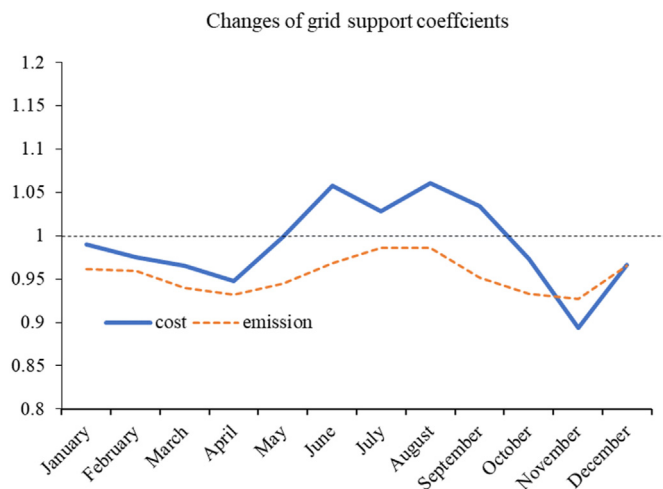


Fig. 16. Changes of grid-support coefficients in each month after scheduling heat pump systems.

PV operation through demand-side management. Individual decision-making towards flexible energy utilization relies heavily on potential electricity cost-saving benefits. Considering the decreasing trend of the renewable feed-in tariff, there would be an increased willingness of the prosumer to shift flexible heat pumps or batteries. Meanwhile, with respect to the increasing distributed energy generators, the offered flexibility of demand-side efforts would be greater. By comparing the residential micro-cogeneration operations of H3 and H4, the output pattern significantly influences their grid-support performance at the system level, and the optimized operational strategy for residential CHP is important at offering grid-support operation. Meanwhile, the waste heat recovery of the fuel cell further increases the carbon emission reduction benefit.

This research is a case study based on the Kyushu grid in Japan, and there are also some limitations. Regarding climate-related variability, the above results may be influenced by the patterns of local electricity consumption and solar irradiation. In addition, depending on the mix of the grid power resources, there would be changes in the grid-support performance of distributed power generation and consumption.

4. Conclusions

To maximize grid renewable penetration while maintaining low electricity costs, the ongoing transformation of a more flexible power system is required. A novel way of exploring the flexibility is to aggregate and manage demand-side energy resources as a grid asset under high renewable penetration. In this work, detailed effects of real-world increases in PV integration on the grid were provided, and the operational scenarios of different existing distributed flexible options were studied using smart meter data obtained from typical Japanese low-carbon residential houses. Further, we examined the grid-support performances of different demand-side flexible options by considering the real-time grid spot price and carbon emission intensity. The findings are summarized as follows:

The increasing share of PV generation has significantly reshaped the pattern of the grid residual load and carbon emission intensity profiles, leading to a negative effect on the value of the real-time spot trading price, and it is more obvious in mid-seasonal months. Meanwhile, the requirement for grid flexibility has also evolved.

The scheduling of existing distributed energy technologies has a strong influence on demand-side flexibility. Specifically, heat pump and battery systems enable promising shiftable loads during the limited hours within a given day with price-responsive requests. The flexible power output of residential cogeneration systems is highly dependent on weather.

The grid-support performances of individual technologies are assessed by the proposed indicators. Given the high penetration of PV production in the public grid, the roles of the grid-tied decentralized PV system in reducing the grid cost and carbon emissions are weakened. The price-responsive scheduling of a heat pump system can result in an obvious cost grid-support performance during the day with a high spot price level. Because its operational time does not coincide with the low grid carbon emission density period, it failed to reduce the carbon emissions at the system level, especially during the mid-season. The grid-supportive performance of residential fuel cell systems depends on the behaviors of occupants. Battery dispatch may lead to a positive cost grid-support operation; however, owing to dispatch energy loss and the low value of carbon emission density difference between the charging and discharging periods, it failed to reduce the carbon emissions at the system level.

An optimal scheduling of a residential heat pump and PV system can improve the grid-support performance, and the combined effects of the demand-side effort are expected to help decarbonize the electricity grid and stabilize its cost-effectiveness operation further. The findings of this work could help policymakers in a more flexible power transition and provide references for efficient public grid design considering demand-side engagement.

Credit author statement

Yanxue Li: Conceptualization; Methodology; Software; Validation; Investigation; Formal analysis; Writing – original draft; Visualization. : Investigation; Data curation. & : Software. : Project administration; Funding acquisition; Conceptualization; Methodology.

Declaration of competing interest

The authors declare that they have no known competing financial interests or personal relationships that could have appeared to influence the work reported in this paper.

Acknowledgements

This research was funded by Research on the energy efficiency and health performance improvement of building operations based on lifecycle carbon emissions reduction Grant number 2018YFE0106100 and Development of the Healthy and Low-carbon Residential House with Smart Home Environment Management System, grant number 2019GSF110003. We gratefully acknowledge the help from ASSURAN International Scholarship Foundation.

Appendix A. . Daily average grid market spot trading price in each month, Yen/kWh

Times	January	February	March	April	May	June	July	August	September	October	November	December
0:00	7.49	6.08	5.31	6.03	6.30	6.15	5.58	5.53	5.70	6.08	5.32	6.26
1:00	7.64	6.50	5.54	6.83	6.59	6.26	5.47	5.08	5.69	6.22	5.90	6.54
2:00	7.60	6.63	5.72	7.65	7.21	6.82	5.55	5.01	5.94	6.70	6.74	6.81
3:00	7.45	6.42	5.72	7.66	7.39	6.98	5.74	5.13	6.20	6.90	6.96	6.85
4:00	7.74	6.50	5.85	7.76	7.34	6.69	5.84	5.54	6.31	6.98	7.04	7.02
5:00	8.67	7.66	6.79	7.23	6.25	6.01	5.80	5.38	6.13	7.13	7.70	7.96
6:00	10.04	8.30	6.72	6.01	5.13	5.75	5.86	5.99	5.98	6.68	7.16	8.97
7:00	9.53	7.94	6.38	5.97	4.95	6.24	6.02	6.61	6.65	6.76	6.56	8.31
8:00	9.11	7.89	6.13	6.18	5.33	7.03	6.57	7.27	7.39	6.76	5.84	7.63
9:00	7.59	6.60	5.11	4.98	4.65	6.69	6.64	7.60	7.29	6.09	3.90	6.44
10:00	6.82	5.90	4.39	5.01	4.64	6.91	6.91	7.96	7.52	6.00	2.86	5.31
11:00	5.63	4.68	2.92	3.58	3.74	5.77	5.99	7.40	6.79	4.88	2.10	4.39
12:00	6.29	5.26	3.86	5.05	5.32	7.21	6.91	8.23	7.98	6.42	3.50	5.02
13:00	6.69	5.54	4.28	5.45	5.87	7.57	7.20	8.99	9.10	7.45	5.53	5.80
14:00	7.30	5.90	4.85	6.19	6.44	7.77	7.64	11.39	10.30	8.31	6.73	6.84
15:00	8.82	7.15	5.77	6.84	7.41	8.55	8.49	14.30	12.90	10.01	8.37	8.65
16:00	10.21	8.33	6.78	7.98	8.03	8.56	8.52	12.70	14.48	10.98	9.72	10.36
17:00	10.64	8.87	7.88	9.29	9.15	8.97	8.90	14.39	15.46	10.58	9.41	9.85
18:00	9.75	8.33	7.46	9.27	9.53	9.08	8.70	12.16	11.35	9.12	8.52	9.21
19:00	9.30	8.05	7.04	8.79	8.50	8.44	8.14	10.03	9.31	8.37	8.01	8.82
20:00	8.76	7.53	6.49	8.06	7.78	7.90	7.10	8.52	7.87	7.88	7.46	8.25
21:00	8.94	7.72	6.80	7.48	7.25	7.55	7.33	8.18	7.64	7.48	7.30	8.00
22:00	8.27	6.84	5.76	7.32	6.99	6.93	6.02	7.32	7.20	6.75	6.27	7.28
23:00	7.87	6.19	5.49	6.68	6.65	6.28	5.85	6.61	6.45	6.34	5.37	6.42

Appendix B. . Daily average grid load in each month, MWh

Time	January	February	March	April	May	June	July	August	September	October	November	December
0:00	9352.9	9069.1	8356.8	7569.5	7073.9	7411.0	8126.6	8367.0	7898.1	7169.8	7487.3	8619.8
1:00	9760.1	9510.6	8845.8	8050.6	7433.1	7614.7	8182.0	8327.1	7952.5	7424.3	7945.6	9104.4
2:00	10075.1	9871.2	9313.1	8610.4	8000.3	8096.3	8548.5	8557.7	8297.4	7960.5	8560.4	9575.5
3:00	10190.1	10021.7	9525.9	8877.5	8345.9	8482.2	8893.3	8831.9	8640.9	8351.4	8869.9	9741.5
4:00	10210.9	10026.6	9487.7	8793.6	8245.8	8450.7	8929.5	8950.9	8728.2	8347.9	8810.6	9708.8
5:00	10627.4	10390.4	9652.7	8668.0	7935.6	8246.2	8868.9	8951.2	8640.5	8155.0	8775.5	9931.9
6:00	11250.3	10938.3	9855.3	8588.8	7889.7	8387.3	9279.5	9496.6	8933.2	8227.6	8934.0	10399.3
7:00	11703.5	11251.5	9988.3	8679.4	8203.5	8984.4	10267.0	10571.2	9775.5	8596.5	8931.2	10708.9
8:00	11505.4	11309.1	9974.5	8988.7	8728.3	9716.5	11176.7	11561.8	10687.7	9160.6	9127.2	10718.6
9:00	10975.4	10951.8	9775.7	9058.6	9001.6	10079.4	11584.5	11991.0	11182.2	9475.7	9073.3	10415.2
10:00	10684.5	10710.4	9728.8	9197.8	9249.4	10358.0	11859.1	12314.7	11550.8	9715.6	9117.0	10247.1
11:00	10251.7	10288.8	9358.8	8898.1	9056.6	10137.7	11658.3	12265.7	11428.0	9468.4	8785.0	9818.6
12:00	10254.3	10340.9	9448.4	9050.8	9272.7	10424.8	11915.6	12484.9	11726.7	9726.4	8950.9	9886.4
13:00	10147.1	10206.1	9290.6	8976.9	9263.2	10428.3	11959.2	12530.3	11793.8	9734.5	8925.5	9833.9
14:00	10195.4	10127.6	9231.9	8895.8	9211.8	10378.7	11903.1	12477.3	11741.9	9699.3	8949.0	9912.1
15:00	10652.3	10412.0	9480.4	9024.6	9267.4	10361.9	11967.5	12540.1	11829.9	9821.0	9257.0	10323.2
16:00	11399.9	10936.8	9791.2	9168.8	9270.2	10233.0	11824.6	12408.4	11692.1	9883.3	9739.8	10994.4
17:00	11975.5	11565.1	10321.3	9450.6	9269.1	10150.5	11682.0	12270.1	11659.6	10022.9	9940.9	11280.5
18:00	11814.6	11465.3	10410.3	9557.3	9264.5	10005.4	11458.6	12014.1	11321.1	9620.9	9662.0	11040.5
19:00	11471.0	11114.8	10127.7	9242.6	8907.2	9638.5	10991.4	11410.4	10692.5	9138.7	9305.0	10695.7
20:00	11005.5	10645.9	9711.0	8831.1	8498.2	9131.3	10455.3	10787.1	10082.3	8662.3	8921.7	10240.2
21:00	10414.0	10061.1	9244.3	8438.7	8117.6	8727.1	9903.5	10196.2	9553.7	8290.5	8517.0	9757.0
22:00	9819.1	9485.9	8721.1	8003.3	7711.8	8280.1	9335.4	9584.3	9024.9	7919.6	8116.9	9267.1
23:00	9270.258	8937.929	8212.645	7538.2	7206.613	7665.2	8594.258	8779.613	8300.5	7383.903	7616.967	8716.065

Appendix C. . Daily PV production in each month, MWh

Time	January	February	March	April	May	June	July	August	September	October	November	December
0:00	0.0	0.0	0.4	0.0	0.0	0.0	0.0	0.0	0.0	0.0	0.0	0.0
1:00	0.0	0.0	0.4	0.0	0.0	0.0	0.0	0.0	0.0	0.0	0.0	0.0
2:00	0.0	0.0	0.3	0.0	0.0	0.0	0.0	0.0	0.0	0.0	0.0	0.0
3:00	0.0	0.0	0.3	0.0	0.0	0.0	0.0	0.0	0.0	0.0	0.0	0.0
4:00	0.0	0.0	0.3	1.8	52.4	69.0	24.2	5.9	0.0	0.0	0.0	0.0
5:00	0.0	0.0	37.0	257.7	605.7	567.1	336.9	253.1	169.1	48.5	5.8	0.0
6:00	68.5	138.9	620.5	1184.8	1646.8	1390.4	1025.6	1007.4	1000.9	762.7	441.0	115.4
7:00	757.3	853.5	1744.4	2395.7	2843.4	2340.8	1831.6	1897.0	2126.9	1927.4	1522.2	813.7
8:00	1769.5	1853.8	2940.4	3579.4	3913.2	3150.6	2630.1	2776.4	3133.2	3101.9	2796.6	1783.6
9:00	2796.4	2746.0	3864.0	4379.7	4664.3	3813.7	3246.1	3404.8	3853.5	4020.4	3655.9	2621.3
10:00	3455.2	3317.3	4464.0	4879.0	5107.4	4225.7	3638.5	3776.6	4276.6	4461.2	4195.8	3148.2
11:00	3593.7	3573.9	4663.0	4994.1	5174.2	4371.4	3739.5	3888.5	4330.9	4421.5	4243.6	3207.5
12:00	3273.8	3387.6	4503.4	4687.8	4872.1	4202.0	3560.2	3631.5	4023.4	3988.4	3864.2	2924.6
13:00	2711.5	2959.8	3917.1	4088.5	4300.1	3668.8	3180.4	3192.5	3389.1	3196.4	3059.3	2224.3
14:00	1805.5	2242.4	3008.8	3189.0	3484.7	2950.3	2594.7	2541.7	2471.0	2189.4	1815.9	1292.0
15:00	736.7	1184.0	1819.7	1982.7	2350.5	2039.0	1851.4	1734.1	1430.3	1005.4	551.9	378.8
16:00	60.6	251.2	624.7	823.0	1176.3	1137.2	986.0	859.1	473.6	131.1	12.1	4.4
17:00	0.0	0.6	33.7	90.8	272.6	366.7	304.5	181.1	24.4	0.0	0.1	0.1
18:00	0.0	0.0	0.4	0.0	1.4	14.3	11.9	1.5	0.0	0.0	0.0	0.0
19:00	0.0	0.0	0.4	0.0	0.1	0.0	0.0	0.0	0.0	0.0	0.0	0.0
20:00	0.0	0.0	0.4	0.0	0.0	0.0	0.0	0.0	0.0	0.0	0.0	0.0
21:00	0.0	0.0	0.4	0.0	0.1	0.0	0.0	0.0	0.0	0.0	0.0	0.0
22:00	0.0	0.0	0.4	0.0	0.1	0.0	0.0	0.0	0.0	0.0	0.0	0.0
23:00	0.0	0.0	0.5	0.0	0.0	0.0	0.0	0.0	0.0	0.0	0.0	0.0

Appendix D. . Daily grid electricity carbon emission intensity in each month, kg/kWh

Time	January	February	March	April	May	June	July	August	September	October	November	December
0:00	0.44	0.43	0.36	0.35	0.37	0.42	0.41	0.49	0.52	0.48	0.46	0.50
1:00	0.44	0.43	0.36	0.35	0.37	0.42	0.41	0.49	0.52	0.48	0.46	0.48
2:00	0.44	0.43	0.36	0.33	0.36	0.42	0.41	0.48	0.51	0.48	0.45	0.48
3:00	0.44	0.42	0.35	0.33	0.35	0.40	0.42	0.48	0.50	0.46	0.45	0.47
4:00	0.44	0.42	0.35	0.33	0.35	0.40	0.41	0.48	0.50	0.46	0.45	0.47
5:00	0.44	0.42	0.35	0.32	0.34	0.39	0.40	0.47	0.49	0.46	0.44	0.47
6:00	0.42	0.41	0.33	0.30	0.30	0.36	0.39	0.45	0.46	0.43	0.43	0.45
7:00	0.41	0.39	0.30	0.26	0.27	0.34	0.37	0.42	0.42	0.39	0.38	0.43
8:00	0.37	0.36	0.25	0.22	0.25	0.31	0.35	0.40	0.39	0.35	0.33	0.40
9:00	0.33	0.32	0.22	0.21	0.23	0.30	0.33	0.38	0.37	0.32	0.30	0.38
10:00	0.30	0.29	0.21	0.20	0.22	0.29	0.33	0.37	0.36	0.31	0.28	0.36
11:00	0.29	0.28	0.20	0.20	0.22	0.29	0.32	0.38	0.37	0.31	0.28	0.35
12:00	0.31	0.30	0.21	0.21	0.23	0.29	0.33	0.38	0.37	0.33	0.30	0.37
13:00	0.34	0.32	0.22	0.22	0.24	0.30	0.34	0.39	0.39	0.35	0.34	0.39
14:00	0.37	0.35	0.24	0.24	0.26	0.32	0.36	0.41	0.41	0.39	0.39	0.43
15:00	0.42	0.39	0.28	0.27	0.29	0.35	0.38	0.43	0.44	0.42	0.43	0.47
16:00	0.43	0.41	0.33	0.31	0.33	0.38	0.41	0.46	0.47	0.43	0.44	0.46
17:00	0.42	0.41	0.35	0.33	0.35	0.39	0.42	0.47	0.48	0.43	0.43	0.46
18:00	0.43	0.42	0.35	0.33	0.35	0.40	0.43	0.48	0.49	0.45	0.44	0.47
19:00	0.44	0.42	0.35	0.34	0.35	0.41	0.43	0.49	0.50	0.47	0.45	0.47
20:00	0.45	0.43	0.36	0.34	0.36	0.42	0.43	0.49	0.51	0.47	0.46	0.48
21:00	0.45	0.43	0.36	0.34	0.36	0.42	0.43	0.49	0.51	0.48	0.46	0.48
22:00	0.44	0.43	0.36	0.35	0.37	0.43	0.42	0.49	0.51	0.47	0.46	0.48
23:00	0.44	0.43	0.36	0.35	0.37	0.42	0.42	0.48	0.51	0.48	0.46	0.50

References

[1] Gielen D, Boshell F, Saygin D, Bazilian MD, Wagner N, Gorini R. The role of renewable energy in the global energy transformation. *Energy Strategy Reviews* 2019;24:38–50.
 [2] He G, Lin J, Sifuentes F, Liu X, Abhyankar N, Phadke A. Rapid cost decrease of renewables and storage accelerates the decarbonization of China's power system. *Nat Commun* 2020;11(1):2486.

[3] Newell RG, Raimi D. *Global energy outlook comparison methods: 2020 update*. 2020.
 [4] Simpson J, Loth E, Dykes K. Cost of Valued Energy for design of renewable energy systems. *Renew Energy* 2020;153:290–300.
 [5] Heptonstall PJ, Gross RJK. A systematic review of the costs and impacts of integrating variable renewables into power grids. *Nature Energy* 2020;6(1):72–83.
 [6] Wang D, Muratori M, Eichman J, Wei M, Saxena S, Zhang C. Quantifying the flexibility of hydrogen production systems to support large-scale renewable energy integration. *J Power Sources* 2018;399:383–91.
 [7] Li Y, Gao W, Ruan Y, Ushifusa Y. The performance investigation of increasing

- share of photovoltaic generation in the public grid with pump hydro storage dispatch system, a case study in Japan. *Energy* 2018;164:811–21.
- [8] Li Y, Zhang X, Gao W, Ruan Y. Capacity credit and market value analysis of photovoltaic integration considering grid flexibility requirements. *Renew Energy* 2020;158:908–19.
- [9] Heffron R, Körner M-F, Wagner J, Weibelzahl M, Fridgen G. Industrial demand-side flexibility: a key element of a just energy transition and industrial development. *Appl Energy* 2020;269:115026.
- [10] Broadstock D, Ji Q, Managi S, Zhang D. Pathways to carbon neutrality: challenges and opportunities. *Resour Conserv Recycl* 2021;169:105472.
- [11] Karhunmaa K. Attaining carbon neutrality in Finnish parliamentary and city council debates. *Futures* 2019;109:170–80.
- [12] Mitchell C. Momentum is increasing towards a flexible electricity system based on renewables. *Nature Energy* 2016;1(2).
- [13] Arbabzadeh M, Sioshansi R, Johnson JX, Keoleian GA. The role of energy storage in deep decarbonization of electricity production. *Nat Commun* 2019;10(1):3413.
- [14] O'Dwyer C, Flynn D. Impact of flexibility service requirements on investment decisions and costs. 2019.
- [15] Harder N, Qussous R, Weidlich A. The cost of providing operational flexibility from distributed energy resources. *Appl Energy* 2020;279:115784.
- [16] Backe S, Korpås M, Tomasgard A. Heat and electric vehicle flexibility in the European power system: a case study of Norwegian energy communities. *Int J Electr Power Energy Syst* 2021;125:106479.
- [17] Kumamoto T, Aki H, Ishida M. Provision of grid flexibility by distributed energy resources in residential dwellings using time-of-use pricing. *Sustainable Energy, Grids and Networks* 2020;23:100385.
- [18] Fitzpatrick P, D'Ettoire F, De Rosa M, Yadack M, Eicker U, Finn DP. Influence of electricity prices on energy flexibility of integrated hybrid heat pump and thermal storage systems in a residential building. *Energy Build* 2020;223:110142.
- [19] Li Y, Gao W, Ruan Y, Ushifusa Y. Grid load shifting and performance assessments of residential efficient energy technologies, a case study in Japan. *Sustainability* 2018;10(7):2117.
- [20] Wanapinit N, Thomsen J, Kost C, Weidlich A. An MILP model for evaluating the optimal operation and flexibility potential of end-users. *Appl Energy* 2021;282:116183.
- [21] Cole W, Frazier A. Cost projections for utility-scale battery storage: 2020 update. National Renewable Energy Lab.(NREL) 2020:1–13. Golden, CO (United States).
- [22] Ruhnau O, Hirth L, Praktikno A. Heating with wind: economics of heat pumps and variable renewables. *Energy Econ* 2020;92:104967.
- [23] Hirth L, Ueckerdt F, Edenhofer O. Integration costs revisited – an economic framework for wind and solar variability. *Renew Energy* 2015;74:925–39.
- [24] Hirth L. The market value of variable renewables. *Energy Econ* 2013;38:218–36.
- [25] Hirth L. The benefits of flexibility: the value of wind energy with hydropower. *Appl Energy* 2016;181:210–23.
- [26] Muratori M. Impact of uncoordinated plug-in electric vehicle charging on residential power demand. *Nature Energy* 2018;3(3):193–201.
- [27] Reimuth A, Prasch M, Locherer V, Danner M, Mauser W. Influence of different battery charging strategies on residual grid power flows and self-consumption rates at regional scale. *Appl Energy* 2019;238:572–81.
- [28] Rehman OU, Khan SA, Javaid N. Impact of photovoltaic self-consumption curtailment on building-to-grid operations. *Int J Electr Power Energy Syst* 2021;124:106374.
- [29] Katz J, Andersen FM, Morthorst PE. Load-shift incentives for household demand response: evaluation of hourly dynamic pricing and rebate schemes in a wind-based electricity system. *Energy* 2016;115:1602–16.
- [30] Dehnavi E, Abdi H. Optimal pricing in time of use demand response by integrating with dynamic economic dispatch problem. *Energy* 2016;109:1086–94.
- [31] Stelmach G, Zanocco C, Flora J, Rajagopal R, Boudet HS. Exploring household energy rules and activities during peak demand to better determine potential responsiveness to time-of-use pricing. *Energy Pol* 2020;144:111608.
- [32] Mehrjerdi H, Hemmati R. Coordination of vehicle-to-home and renewable capacity resources for energy management in resilience and self-healing building. *Renew Energy* 2020;146:568–79.
- [33] Li Y, Gao W, Zhang X, Ruan Y, Ushifusa Y, Hirotsu F. Techno-economic performance analysis of zero energy house applications with home energy management system in Japan. *Energy Build* 2020;214:109862.
- [34] Klein K, Herkel S, Henning H-M, Felsmann C. Load shifting using the heating and cooling system of an office building: quantitative potential evaluation for different flexibility and storage options. *Appl Energy* 2017;203:917–37.
- [35] Jensen SØ, Marszal-Pomianowska A, Lollini R, Pasut W, Knotzer A, Engelmann P, et al. IEA EBC annex 67 energy flexible buildings. *Energy Build* 2017;155:25–34.
- [36] Roth A, Reyna J. Grid-interactive efficient buildings technical report series: whole-building controls, sensors, modeling, and analytics. National Renewable Energy Lab.(NREL) 2019;1:1–51. Golden, CO (United States).
- [37] Eckman T, Schwartz LC, Leventis G. Determining utility system value of demand flexibility from grid-interactive efficient buildings. 2020.
- [38] Kotarela F, Kyritsis A, Papanikolaou N, Kalogirou SA. Enhanced nZEB concept incorporating a sustainable Grid Support Scheme. *Renew Energy* 2021;169:714–25.
- [39] Fosas D, Nikolaidou E, Roberts M, Allen S, Walker I, Coley D. Towards active buildings: rating grid-servicing buildings. *Build Serv Eng Technol* 2020:014362442097464.
- [40] Aguilar-Dominguez D, Dunbar A, Brown S. The electricity demand of an EV providing power via vehicle-to-home and its potential impact on the grid with different electricity price tariffs. *Energy Rep* 2020;6:132–41.
- [41] Lazzeroni P, Olivero S, Repetto M, Stirano F, Vallet M. Optimal battery management for vehicle-to-home and vehicle-to-grid operations in a residential case study. *Energy* 2019;175:704–21.
- [42] Jimenez-Navarro J-P, Kavvadias K, Filippidou F, Pavičević M, Quoilin S. Coupling the heating and power sectors: the role of centralised combined heat and power plants and district heat in a European decarbonised power system. *Appl Energy* 2020;270:115134.
- [43] Brown T, Schlachtberger D, Kies A, Schramm S, Greiner M. Synergies of sector coupling and transmission reinforcement in a cost-optimised, highly renewable European energy system. *Energy* 2018;160:720–39.
- [44] Li Y, Gao W, Ruan Y. Performance investigation of grid-connected residential PV-battery system focusing on enhancing self-consumption and peak shaving in Kyushu, Japan. *Renew Energy* 2018;127:514–23.
- [45] Frazier AW, Cole W, Denholm P, Greer D, Gagnon P. Assessing the potential of battery storage as a peaking capacity resource in the United States. *Appl Energy* 2020;275:115385.
- [46] Jaglal D, Procopiou AT, Petrou K, Ochoa LF. Bottom-up modeling of residential batteries and their effect on system-level generation cost. *Elec Power Syst Res* 2020;189:106711.
- [47] Hungerford Z, Bruce A, MacGill I. The value of flexible load in power systems with high renewable energy penetration. *Energy* 2019;188:115960.
- [48] Fischer D, Wolf T, Wapler J, Hollinger R, Madani H. Model-based flexibility assessment of a residential heat pump pool. *Energy* 2017;118:853–64.
- [49] Huang P, Lovati M, Zhang X, Bales C, Hallbeck S, Becker A, et al. Transforming a residential building cluster into electricity prosumers in Sweden: optimal design of a coupled PV-heat pump-thermal storage-electric vehicle system. *Appl Energy* 2019;255:113864.
- [50] Schwarz H, Schermeyer H, Bertsch V, Fichtner W. Self-consumption through power-to-heat and storage for enhanced PV integration in decentralised energy systems. *Sol Energy* 2018;163:150–61.
- [51] Vijay A, Hawkes A. Demand side flexibility from residential heating to absorb surplus renewables in low carbon futures. *Renew Energy* 2019;138:598–609.
- [52] Nyttén T, Claessens B, Paredis K, Van Bael J, Six D. Flexibility of a combined heat and power system with thermal energy storage for district heating. *Appl Energy* 2013;104:583–91.
- [53] De Rosa M, Carragher M, Finn DP. Flexibility assessment of a combined heat-power system (CHP) with energy storage under real-time energy price market framework. *Thermal Science and Engineering Progress* 2018;8:426–38.
- [54] Takeshita T, Aki H, Kawajiri K, Ishida M. Assessment of utilization of combined heat and power systems to provide grid flexibility alongside variable renewable energy systems. *Energy* 2021;214:118951.
- [55] Sandberg E, Kirkerud JG, Trømborg E, Bolkesjø TF. Energy system impacts of grid tariff structures for flexible power-to-district heat. *Energy* 2019;168:772–81.
- [56] Tang H, Wang S. Energy flexibility quantification of grid-responsive buildings: energy flexibility index and assessment of their effectiveness for applications. *Energy* 2021;221:119756.
- [57] Zhang X, Gao W, Li Y, Wang Z, Ushifusa Y, Ruan Y. Operational performance and load flexibility analysis of Japanese zero energy house. *Int J Environ Res Publ Health* 2021;18(13):6782.
- [58] Huang S, Ye Y, Wu D, Zuo W. An assessment of power flexibility from commercial building cooling systems in the United States. *Energy* 2021;221:119571.
- [59] Impram S, Varbak Nese S, Oral B. Challenges of renewable energy penetration on power system flexibility: a survey. *Energy Strategy Reviews* 2020;31:100539.
- [60] Battaglia M, Haberl R, Bamberger E, Haller M. Increased self-consumption and grid flexibility of PV and heat pump systems with thermal and electrical storage. *Energy Procedia* 2017;135:358–66.
- [61] Reynders G, Diriken J, Saelens D. Generic characterization method for energy flexibility: applied to structural thermal storage in residential buildings. *Appl Energy* 2017;198:192–202.
- [62] Zhang C, Greenblatt JB, Wei M, Eichman J, Saxena S, Muratori M, et al. Flexible grid-based electrolysis hydrogen production for fuel cell vehicles reduces costs and greenhouse gas emissions. *Appl Energy* 2020;278:115651.
- [63] Hu M, Xiao F. Quantifying uncertainty in the aggregate energy flexibility of high-rise residential building clusters considering stochastic occupancy and occupant behavior. *Energy* 2020;194:116838.
- [64] Bistline J, Cole W, Damato G, DeCarolis J, Frazier W, Linga V, et al. Energy storage in long-term system models: a review of considerations, best practices, and research needs. *Progress in Energy* 2020;2(3):32001.
- [65] Institute JRE. Power supply and demand chart. 2020.
- [66] Institute RE. Power supply & demand chart, JEPX day-ahead market price. 2020.
- [67] Klein K, Langner R, Kalz D, Herkel S, Henning H-M. Grid support coefficients for electricity-based heating and cooling and field data analysis of present-day installations in Germany. *Appl Energy* 2016;162:853–67.
- [68] Panasonic. Residential fuel cell cogeneration system. 2020.